Article

Synthetic Minority Oversampling Enhanced FEM for Tool Wear Condition Monitoring

Yuqing Zhou [1,2], Canyang Ye [3], Deqiang Huang [3], Bihui Peng [3], Bintao Sun [2,*] and Huan Zhang [4,*]

[1] School of Information Science and Technology, Northwest University, Xi'an 710127, China
[2] College of Mechanical and Electrical Engineering, Wenzhou University, Wenzhou 325035, China
[3] Zhejiang Meishuo Electric Technology Co., Ltd., Wenzhou 325699, China
[4] Laser and Optoelectronic Intelligent Manufacturing Research Institute, Wenzhou University, Wenzhou 325025, China
[*] Correspondence: 00131041@wzu.edu.cn (B.S.); ayahuan1018@163.com (H.Z.)

Abstract: Recent advances in artificial intelligence (AI) technology have led to increasing interest in the development of AI-based tool wear condition monitoring methods, heavily relying on large training samples. However, the high cost of tool wear experiment and the uncertainty of tool wear change in the machining process lead to the problems of sample missing and insufficiency in the model training stage, which seriously affects the identification accuracy of many AI models. In this paper, a novel identification method based on finite-element modeling (FEM) and the synthetic minority oversampling technique (SMOTE) is proposed to overcome the problem of sample missing and sample insufficiency. Firstly, a few tool wear monitoring experiments are carried out to obtain experimental samples with low cost. Then, a FEM model based on the Johnson–Cook constitutive model was established and verified according to the experimental samples. Based on the verified FEM model, the simulated missing sample in the experiments can be supplemented to compose a complete training set. Finally, the SMOTE is employed to expand the sample size to construct a perfect training set to train the SVM classification model. End milling tool wear monitoring experiments demonstrate that the proposed FEM-SMOTE method can obtain 98.7% identification accuracy, which is 30% higher than that based on experimental samples. The proposed method provides an effective approach for tool wear condition monitoring with low experimental cost.

Keywords: tool wear condition; sample missing and insufficiency; finite-element modeling; synthetic minority oversampling technique

1. Introduction

Computer numerical control (CNC) machine tools are currently one of the most widely used pieces of processing equipment in the manufacturing industry. Cutting tools are the terminals in direct contact with the processed workpiece in CNC machine tools, and their health condition directly affects the processing quality of the workpiece. In severe cases, they can even damage the machine tool and affect its service life, not only affecting processing efficiency but also increasing production costs. It is the most easily damaged part of the machine tool due to the extrusion and friction with the workpiece in the machining process. According to [1,2], the proportion of machine tool downtime caused by tool health problems in the total downtime can be as high as 20%, and the cost related to tools accounts for 25% of the total processing cost. In addition, the tool wear condition can affect the surface quality of the workpiece and even damage the machine tool in some serious cases [3,4]. Timely and accurate recognition of tool wear condition can greatly reduce the machining cost. Therefore, it is a hot issue to develop an effective online tool condition monitoring (TCM) method in both academia and industry circles [5].

With the development of artificial intelligence (AI), many AI models have been applied to tool wear identification [6], including the hidden Markov model (HMM) [7], support

vector machine (SVM) [8], artificial neural network (ANN) [9,10], and long short-term memory network [11]. For example, Gao et al. [12] employed hybrid stationary subspace analysis and least-squares SVM method for machine tool fault diagnosis using a single vibration sensor. Zhou et al. [1] proposed a TCM method based on a two-layer angle kernel extreme learning machine (KELM) and binary differential evolution for milling. Chen et al. [13] identified the tool condition using a convolutional neural network (CNN) with machine spindle vibration signals. Arellano et al. [14] employed gramian angular summation field algorithm to convert continuous cutting force signals into images and input to a CNN model to detect tool wear condition. Mohanraj et al. [15] summarized various monitoring methods for TCM in the milling process, in which several current AI models are introduced. These AI models provide strong technical support for tool wear identification; however, there is a problem that needs to be solved: sample missing and insufficiency. Due to the complexity of the machining operation, the change of the tool wear condition has certain uncertainty; it is difficult to obtain complete samples of all tool wear conditions in a few experiments, resulting in the problem of sample missing and insufficiency. This problem can be overcome by doing a lot of experiments, but the cost of repeated experiments will significantly increase. Recently, several researchers studied TCM methods to overcome the problem of sample insufficiency. Zhou et al. [16] proposed a phase space reconstruction enhanced multiscale edge-labeling graph neural network (MEGNN) for TCM, which is demonstrated by two TCM experiments under small samples. Milind et al. [17] used a singular generative adversarial network and LSTM to predict tool wear in face milling of stainless steel and obtained very few errors. However, neither SVM, CNN, nor GNN can recognize the categories they have not learned; they cannot solve the problem of missing samples. Although SVM is suitable for small sample learning, the problem of sample imbalance will still significantly affect its classification accuracy [18]. Therefore, a low-cost and easy-to-implement method is needed to solve the problem of sample missing and insufficiency. In recent years, the numerical simulation technology was promoted by the improvement of computer technology; more and more researchers have begun to pay attention to this technology [19,20]. For example, Xiang et al. [21] proposed a personalized diagnosis method of shaft based on numerical simulation combined with wavelet packet transform (WPT) and an SVM model to realize the diagnosis of different shaft faults. Gao et al. [22] solved the problem of missing and insufficient samples of bearing faults by combining finite-element simulation (FEM) and generative adversarial networks (GANs) and provided complete training samples for AI models. As for TCM, no article has been published to carry out the FEM-based method to solve the above problems. In this paper, a novel tool wear condition identification method based on FEM and the synthetic minority oversampling technique (SMOTE) is proposed to solve this problem for tool wear condition identification under low experimental cost.

The main contributions of this article are as follows:

(1) Samples associated with some tool wear conditions are often missing due to the complex conditions encountered in the machining process that lead to the inability of many machine-learning models. To solve the missing and insufficient samples of the real-world machining process, a novel tool wear condition monitoring scheme using FEM and the SMOTE is proposed.

(2) FEM is employed to simulate the hard-to-get wear categories collected from the real-world machining process, and the SMOTE is used to enlarge numerical simulated and physical experimental tool wear samples to generate relatively complete samples.

2. Proposed Method

2.1. Method's Framework

The flowchart of the proposed method is shown in Figure 1, and the four steps of the proposed method are outlined in detail as follows:
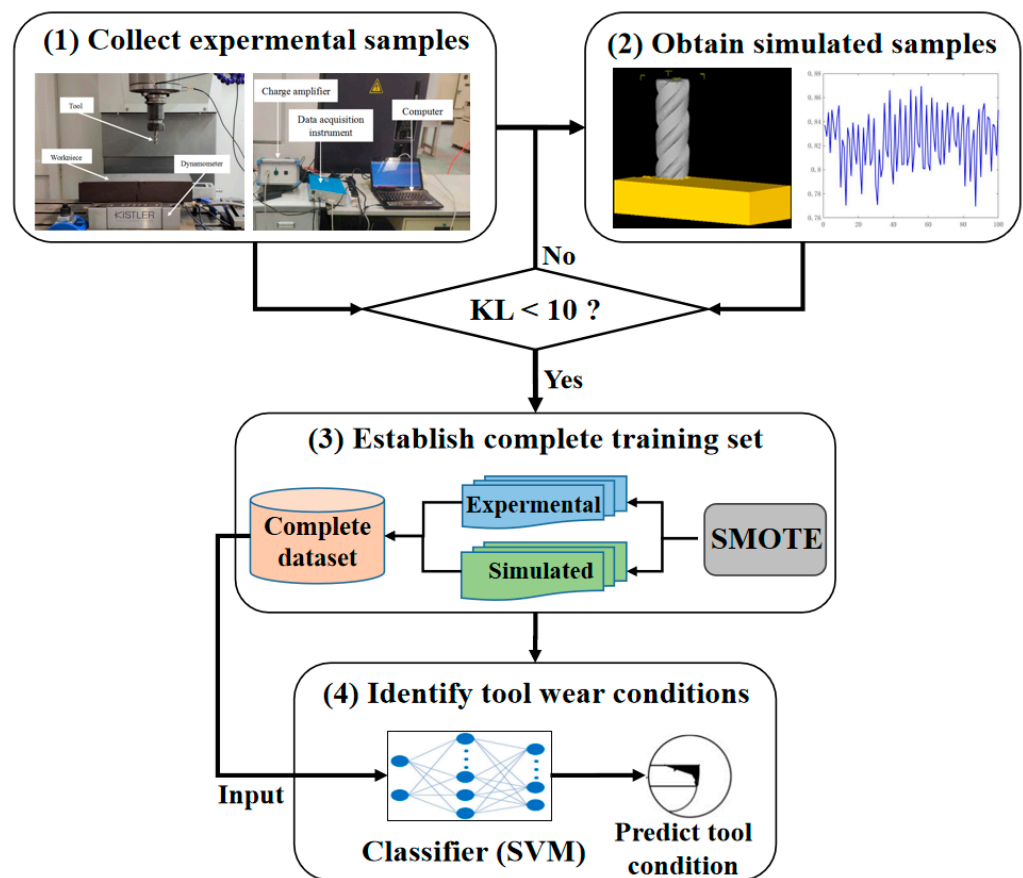
Figure 1. Flowchart of the proposed FEM-SMOTE method.

(1) Collect experimental samples. Carry out a few tool monitoring experiments according to the production situation, collect the cutting force signals in the machining process using a three-component dynamometer, and obtain several experimental samples of different tool wear conditions, as shown in Section 3.1.

(2) Obtain simulated samples through a FEM model. With the help of FEM commercial software (such as Deform V12), a FEM model based on the Johnson–Cook (J-C) constitutive model is established according to the tools, workpiece materials and cutting parameters used in the experiment; the simulated samples are obtained by the FEM model and compared with the experimental samples (shown in Section 2.2). If the signal of the simulated sample and that of the experimental sample are similar, it can be considered that the FEM model is effective. Otherwise, the parameters in the FEM model need to be optimized.

The FEM model can be further modified by model updating or parameter optimization until the Kullback–Leibler (KL) divergence between the simulation data distribution and the measured data distribution is less than 10. Here, the KL divergence measures the difference in the probability distributions of the two groups of signals.

(3) Establish a complete training set. Based on the verified FEM model, the simulated sample of missing tool conditions in the experiments can be supplemented to compose a complete training sample set. Then, the SMOTE is employed to expand the sample size for all tool conditions to construct a perfect training set (shown in Section 2.3), including complete tool conditions and sufficient samples.

(4) Identify tool wear conditions based on a support vector machine (SVM). Several feature parameters in time and frequency domains are extracted, such as average, root mean square (RMS), standard deviation (STD), crest factor, shape factor, skewness, kurtosis, and waveform in the time domain, mean of the power spectrum, RMS of the power spectrum, crest factor of the power spectrum, modified equivalent bandwidth, high-low ratio of the power spectrum, stabilization ratio, skewness, and kurtosis of band power in the frequency

domain (for details, please refer to [20]). These extracted features are used to train an SVM. And the trained SVM model can be applied to identify tool wear condition.

2.2. Finite-Element Method

Finite-element method (FEM) is a numerical technique for solving approximate solutions of boundary value problems [23,24]. Because of the diversity and flexibility, FEM has been expanded and applied in many fields to obtain approximate solutions of various engineering problems [25].

Currently, commonly used commercial FEM software packages include Deform, Abaqus, and Ansys. The preprocessing part of Deform has special cutting modules and rich material library, which provides convenience and professionalism for cutting simulation, and its accuracy has been internationally recognized. Therefore, Deform is applied in this paper to simulate the machining process of the machine tool.

The constitutive equation of metal cutting can reflect the relationship between stress and strain. In the process of metal cutting, the constitutive equation can describe the stress–strain relationship of materials under a large strain rate. In this paper, the Johnson–Cook (J–C) model is employed to describe the material constitutive relationship, as its structure is simple and the influence of temperature change on the material is considered [26].

The J-C constitutive equation is as follows:

$$\sigma = (A + B\varepsilon^n)\left(1 + C\ln\left(\frac{\varepsilon\prime}{\varepsilon_0\prime}\right)\right)\left(1 - \left(\frac{T - T_0}{T_{melt} - T_0}\right)^m\right) \tag{1}$$

where σ denotes the flow stress; ε, ε', and ε_0' denote the plastic strain, strain rate, and reference plastic strain rate, respectively (set 1.0 s^{-1} generally); and T, T_{melt}, and T_0 are the cutting temperature, material melting point, and room temperature (usually 20 degrees), respectively. A is the initial yield stress, B is the strain hardening coefficient, and C is the strain rate sensitivity coefficient. N and M are the strain hardening index and temperature softening index, respectively.

2.3. Synthetic Minority Oversampling Technique

The SMOTE is a new sample expansion method based on a random oversampling algorithm, which can supplement the training data and provide multiple data copies of categories with fewer samples, which is one of the earliest methods proposed and proved to be reliable [27]. Random oversampling is to copy each category with fewer samples and randomly select some of them for replacement. However, the resulting samples will easily lead to model overfitting. The SMOTE increases the sample number by synthesizing samples rather than simply copying samples.

The flow of the SMOTE is as follows:

(1) For each sample x of category C, its K-nearest neighbor is obtained by calculating the Euclidean distance from it to all samples in category C.
(2) Several samples are randomly chosen from the K-nearest neighbors of x, recorded as x_n.
(3) For each x_n, a new synthetic sample is constructed with the original sample x by:

$$x_{new} = x + rand(0,1) \times |x - x_n| \tag{2}$$

where rand (0,1) denotes a random number in the interval (0,1).

Repeat the above steps to generate more samples to achieve the purpose of sample expansion.

2.4. Support Vector Machine

An SVM is a pattern classification algorithm proposed by Vapnik [28]. The development of SVM models is mature, and different software platforms have corresponding algorithm modules with good compatibility and fast speed. Thus, the SVM model is employed here to identify tool wear conditions.

The purpose of the SVM is to find a hyperplane to segment the training data set. The segmentation principle is to maximize the margin, which is finally transformed into a convex quadratic programming problem [12]. The SVM obtains excellent classification accuracy by finding the hyperplane with the maximum margin, that is:

$$\max_{w,b} \frac{2}{\|W\|}$$
$$s.t.\ y_i(\omega^T x_i + b) \geq 1, i = 1, 2, \cdots, m \tag{3}$$

For the convenience of calculation, Equation (3) is transformed into the following:

$$\min_{w,b} \frac{1}{2}\|W\|^2$$
$$s.t.\ y_i(\omega^T x_i + b) \geq 1, i = 1, 2, \cdots, m \tag{4}$$

Equation (4) is the basic type of an SVM. Due to the low requirements for raw data distribution, the SVM has been widely applied and obtained good performance.

3. Experimental Research

3.1. Experimental Setup

The milling experimental platform is built on a machining center (DMTG VDL850A, Dalian Machine Tool Group, Dalian, China), as shown in Figure 2. A Kistler dynamometer (No. 9139AA) is installed below the workpiece to measure the cutting forces in three directions and collect the cutting force signals with 12 kHz sampling frequency using an Avant MI-7016 data acquisition instrument (Econ Technologies Co., Ltd., Hangzhou, China). The workpiece material is AISI 1045 steel, and the size is 300 mm × 100 mm × 80 mm.
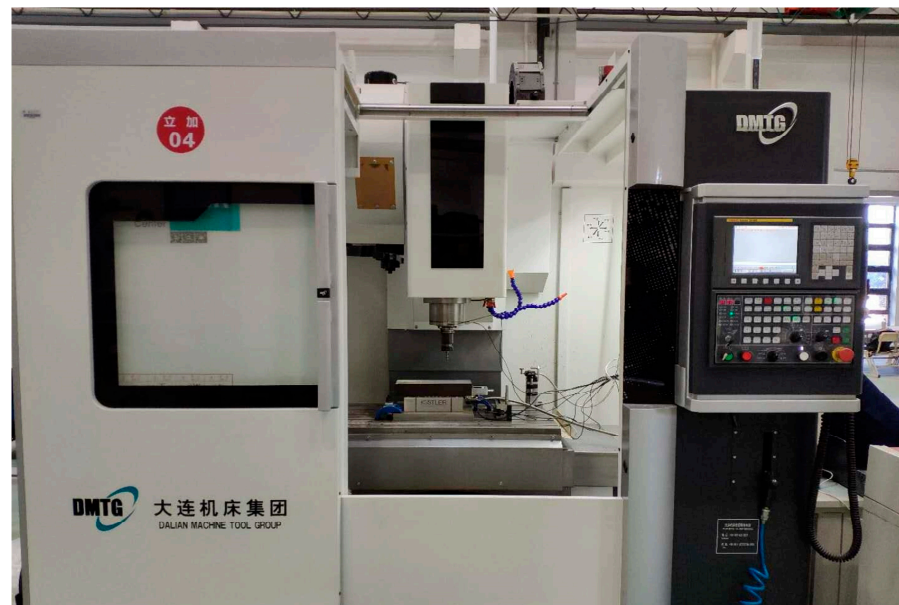
Figure 2. Experimental platform.

Eight uncoated three-edge tungsten steel end-milling tools are applied to finish the milling operation, and each tool corresponds to a certain cutting parameter combination. Three cutting parameters, spindle speed (rpm), depth of cut (mm), and feed rate (mm/min), are set to three levels, as shown in Table 1; for the details, refer to [20]. The wear of each cutting edge of tools was measured offline by a GP-300c tool microscope (Gaopin Precise Instrument Co., Ltd., Suzhou, China) after finishing a workpiece surface, which represented individual milling stages. Each stage included three forward and two backward cuts. Here, the length of rake face wear was employed as the tool wear criterion (shown in [20]), and

the tool wear value after each milling stage was defined as the maximum wear length of the three cutting edges [28].

Table 1. Value of cutting parameters.

Cutting Parameters	Level 1	Level 2	Level 3
Spindle speed (rpm)	2300	2400	2500
Depth of cut (mm)	0.4	0.5	0.6
Feed rate (mm/min)	400	450	500

The maximum value of tool wear in our experiments is 2.054 mm. Therefore, the tool wear condition is divided into seven categories that the interval of each wear category is 0.3 mm, as shown in Table 2. The value in the table represents the sample number in the corresponding wear category; 'No' indicates that there is no sample in the corresponding wear category, that is, the sample is missing. It can be found from Table 2 that there are one or two categories with a missing sample in all tools. Moreover, the sample sizes of each category greatly vary from 5 to 17.

Table 2. Tool wear classifications of the eight tools.

Category	Tool 1	Tool 2	Tool 3	Tool 4	Tool 5	Tool 6	Tool 7	Tool 8
The first category	No	1	No	No	1	No	2	1
The second category	2	1	2	2	2	2	2	1
The third category	2	1	1	2	2	2	3	2
The fourth category	2	3	3	2	3	2	1	1
The fifth category	No	1	1	1	2	1	2	1
The sixth category	2	3	2	3	No	1	No	4
The seventh category	2	No	1	No	No	2	No	No

3.2. FEM Construction

Firstly, the geometric model, boundary conditions, and initial conditions of the FEM model are defined. The dimensions of the workpiece and tool are modeled by SolidWorks V2020 according to the dimensions in the experiment, and imported into Deform. We simplify the simulation model and replace the fixture and other components of the actual machine tool in boundary conditions. Boundary conditions include three cutting elements, constraints between the workpiece and tool, etc. Secondly, the parameters of the J-C model are set. The material library in Deform contains relevant data for about 300 materials. We select AISI 1045 and tungsten steel based on the materials used in the experiment for the workpiece and tool models, respectively. According to the material properties of the experimental workpiece and tool, the parameters in Equation (1) can be set as [29,30]: A = 53.1 Mpa, B = 600.8 MPa, C = 0.0134, n = 0.23, and m = 1. For the friction model, the adhesion occurs in the area near the cutting edge where the tool and chip come into contact, and the frictional shear stress is equal to the average shear flow stress at the tool chip interface in the chip. In the sliding friction zone, the friction shear stress can be calculated by the friction coefficient in the sliding friction between the tool and chip. Therefore, the improved Coulomb friction model is adopted here to better reflect the friction phenomenon between the tool and workpiece, where the friction coefficient is set to 0.6 according to [31].

The meshing numbers of the workpiece and tool are defined as 40,000 and 10,000, respectively. The local refinement ratio is 0.01 on the machined surface. The flow stress under the corresponding strain can be calculated by the friction model and material model, and then the cutting force can be obtained through an integral on the contact surface. Figure 3 shows the simulation process and cutting force data generated.

(**a**) Cutting simulation

(**b**) Cutting force data generated
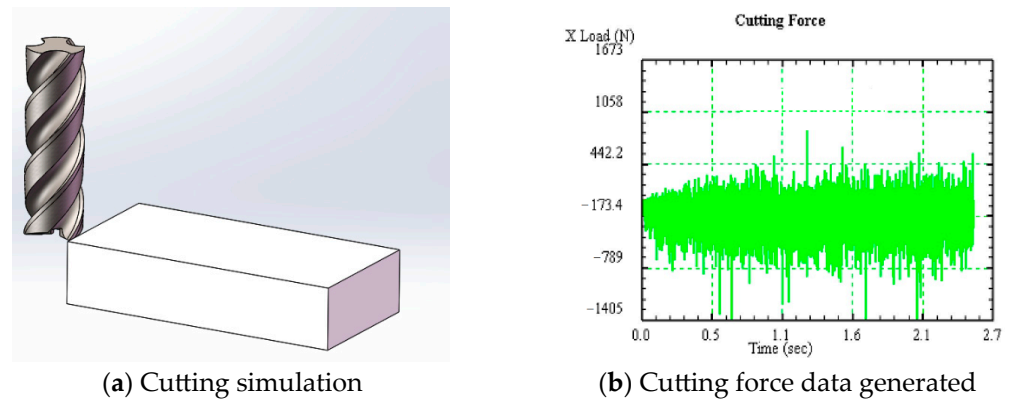
Figure 3. FEM simulation process.

3.3. Verification of Simulation Results

The simulation data can be used as training samples for learning only when they are significantly similar to the experimental data. Here, 1 s (12,000 points) cutting force data of the simulated and experimental signal under the normal condition of the tool are compared to measure their similarity. Since the materials used are common metal materials, a reference value of five parameters in Equation (1) has been suggested in [32,33]. The average KL divergence between the FEM simulated data and experimental data under normal tool conditions is 2.9508, which is lower than the preset threshold. It can be considered that the simulated model is effective. In addition, if the material used is not a commonly used metal material, it is likely that the reference values for the five parameters in Equation (1) are not referenced. It is necessary to select a set of parameter values based on engineering experience and optimize the parameters using orthogonal experimental techniques until the average KL divergence between simulated and experimental data is lower than the preset threshold.

To verify the rationality of the simulated data, the time- and frequency-domain characteristics of the simulated data were compared with the experimental data. Figure 4a shows the time series in the directions of Tool 5, and Figure 4b shows the frequency domain diagram. It can be seen that there is high similarity in time waveform and frequency distribution between the simulated and experimental signals.
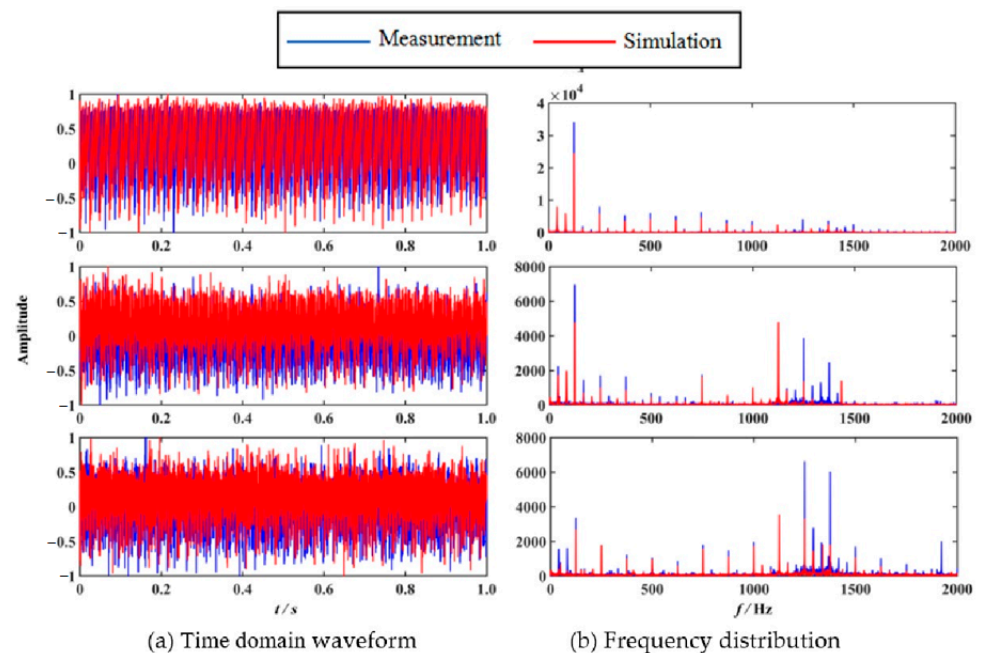
Figure 4. Comparison between simulated and experimental signals.

3.4. Supplement of Missing Sample

Several missing tool conditions in the experiment are artificially added in the FEM model to supply missing samples. Taking Tool 5 as an example, it lacks the sample of the 7th category, and the sample sizes of other categories are different. The tool wear of Tool 5 not measured in the experiment is calculated by a linear interpolation method and then imported into the FEM model to generate simulation samples of the corresponding category [20].

4. Discussion

Due to the length of the paper, the missing samples of the 1st category are not discussed here. According to Table 2, we take Tools 2, 4, 5, 7, and 8 as the training set because the data of their 7th wear category are missing. Therefore, the other three tools (1, 3, and 6) are used as the testing set. The FEM model is employed to establish the complete training set by simulating samples of missing categories in the original training set. Thus, the sample size of experimental, simulated, and completed (experiment + simulation) training sets are 900, 300, and 1200, respectively. In addition, the sample sizes of all categories in each training tool are expanded to 100 through the SMOTE, in which the number of neighbors k is set to 5 according to [33]. Finally, the sample size of experimental, completed, experiment + SMOTE, and perfect (experiment + simulation + SMOTE) training sets are 900, 1200, 4500, and 6000, respectively.

Several feature parameters in time and frequency domains [20,31,34] are extracted, such as average, RMS, STD, crest factor, shape factor, skewness, kurtosis, and waveform in the time domain, mean of the power spectrum, RMS of the power spectrum, crest factor of the power spectrum, modified equivalent bandwidth, high-low ratio of the power spectrum, stabilization ratio, skewness, and kurtosis of bandpower in the frequency domain. These extracted features are used to train the SVM model; the radial basis kernel (RBK) function is selected as the kernel function, and the kernel parameter σ is optimized using a fast leave-one-out cross-validation optimization proposed in [32]; the optimal kernel parameter σ is 2.78.

The classification results are shown in Table 3, in which the classification accuracy of each category and the overall accuracy are defined as follows:

$$Accuracy\ of\ the\ i-th\ category = \frac{True\ positives\ in\ the\ i-th\ category}{Sample\ size\ of\ the\ i-th\ category}$$

$$Overall\ accuracy\ = \frac{\sum\limits_{i=2}^{7} True\ positives\ in\ the\ i-th\ category}{\sum\limits_{i=2}^{7} Sample\ size\ of\ the\ i-th\ category} \tag{5}$$

Table 3. Classification accuracy of different training set.

Training Set		Experiment	Completed	Experiment + SMOTE	Perfection
Sample Size		**900**	**1200**	**4500**	**6000**
	2nd (120)	100.0%	100.0%	100.0%	100.0%
	3rd (100)	56.0%	87.0%	100.0%	100.0%
Testing set:	4th (140)	97.9%	97.9%	100.0%	100.0%
category	5th (40)	95.0%	97.5%	100.0%	100.0%
(sample size)	6th (100)	61.0%	95.0%	93.0%	98.0%
	7th (80)	0.0%	82.5%	0.0%	93.8%
	Overall accuracy	71.0%	93.8%	85.0%	98.8%

It can be found that the classification accuracy based on the completed training set is 22.8% higher than that based on the experimental training set. It can be considered that the simulation samples generated by the FEM mode can effectively solve the problem of sample missing. The classification accuracy based on the experiment + SMOTE training set can get 85% and is 14% higher than the one based on the experimental training set.

Thus, the expanded samples generated by the SMOTE can reduce the impact of insufficient samples on classification models. However, it is 13.8% less than the one based on the perfect training sets. The reason is that AI classification models cannot identify the category they have not learned.

5. Conclusions

This paper proposed a novel tool wear condition identification method based on FEM and the SMOTE to overcome sample missing and insufficiency occurring in practical experiments. Firstly, a few tool wear monitoring experiments are carried out to obtain experimental samples with low cost. Then, a FEM model based on the Johnson–Cook constitutive model was established and verified according to the experimental samples. Based on the verified FEM model, the simulated missing sample in the experiments can be supplemented to compose a complete training set. Finally, the SMOTE is employed to expand the sample size to construct a perfect training set to train the SVM model. End-milling tool wear monitoring experiments demonstrate that the proposed FEM-SMOTE method can obtain good classification accuracy with a small number of experiments at low cost.

Next, there are three aspects worth further exploration:

(1) The cutting force signal used in this paper can be directly obtained through the FEM method. However, the simulation performance of other signals, such as vibration and acoustic emissions, still needs to be studied to explore other effective approaches in TCM methods.
(2) The methods and technologies proposed in this paper are established in a laboratory environment and have not been applied in actual machining processes. Therefore, a TCM online monitoring system can be considered in combination with hardware and software development.
(3) In this article, commonly used metal materials are used in the experiment, and the parameters of the FEM model have reference values. For uncommon useful metal materials, although orthogonal experimental techniques can theoretically be used to find the optimal parameters that meet the threshold, further research is still needed.

Author Contributions: Conceptualization, Y.Z.; methodology and software, C.Y.; validation, D.H. and B.P.; formal analysis, D.H.; investigation, B.P.; resources, H.Z.; writing—original draft preparation, C.Y.; writing—review and editing, B.S.; project administration, B.S. and H.Z.; funding acquisition, H.Z. All authors have read and agreed to the published version of the manuscript.

Data Availability Statement: Not applicable.

Abbreviations

Abbreviation	Term
CNC	Computer numerical control
TCM	Tool wear condition monitoring
AI	Artificial intelligence
HMM	Hidden Markov model
SVM	Support vector machine
KELM	Kernel extreme learning machine
ANN	Artificial neural network
LSTM	Long short–term memory network
WPT	Wavelet packet transform
CNN	Convolutional neural network

GNN	Graph neural network
FEM	Finite-element modeling
GANs	Generative adversarial networks
SMOTE	Synthetic minority oversampling technique
J–C model	Johnson–Cook constitutive model
KL divergence	Kullback–Leibler divergence
RBK	Radial basis kernel
RMS	Root mean square
STD	Standard deviation

References

1. Zhou, Y.Q.; Sun, B.T.; Sun, W.F.; Lei, Z. Tool Wear Condition Monitoring Based on a Two-layer Angle Kernel Extreme Learning Machine using Sound Sensor for Milling Process. *J. Intell. Manuf.* **2022**, *33*, 247–258. [CrossRef]
2. Zheng, G.X.; Chen, W.; Qian, Q.J.; Kumar, A.; Sun, W.; Zhou, Y. TCM in milling processes based on attention mechanism-combined long short-term memory using a sound sensor under different working conditions. *Int. J. Hydromech.* **2022**, *5*, 243–259. [CrossRef]
3. Asif, I.; Zhao, G.L.; Cheok, Q.; He, N.; Nauman, M.M. Sustainable Machining: Tool Life Criterion Based on Work Surface Quality. *Processes* **2022**, *10*, 1087.
4. Najm, S.M.; Paniti, I. Predict the Effects of Forming Tool Characteristics on Surface Roughness of Aluminum Foil Components Formed by SPIF Using ANN and SVR. *Int. J. Precis. Eng. Manuf.* **2021**, *22*, 13–26. [CrossRef]
5. Zhou, Y.Q.; Sun, W.; Ye, C.Y.; Peng, B.; Fang, X.; Lin, C.; Wang, G.; Kumar, A.; Sun, W.F. Time-frequency Representation -enhanced Transfer Learning for Tool Condition Monitoring during milling of Inconel 718. *Eksploat. Niezawodn.—Maint. Reliab.* **2023**, *25*, 165926. [CrossRef]
6. Jung, S.; Kim, M.; Kim, B.; Kim, J.; Kim, E.; Kim, J.; Lee, H.; Kim, S. Fault Detection for CNC Machine Tools Using Auto-Associative Kernel Regression Based on Empirical Mode Decomposition. *Processes* **2022**, *10*, 2529. [CrossRef]
7. Govind, V.; Kumar, R. An amended grey wolf optimization with mutation strategy to diagnose bucket defects in Pelton wheel. *Measurement* **2021**, *187*, 110272.
8. Kothuru, A.; Nooka, S.P.; Liu, R. Application of audible sound signals for tool wear monitoring using machine learning techniques in end milling. *Int. J. Adv. Manuf. Technol.* **2018**, *95*, 3797–3808. [CrossRef]
9. Wang, H.C.; Su, W.; Sun, W.F.; Ren, Y.; Zhou, Y.; Qian, Q.; Kumar, A. A novel tool condition monitoring based on Gramian angular field and comparative learning. *Int. J. Hydromechatron.* **2023**, *6*, 93–107. [CrossRef]
10. Johanna, M.F.; José, V.A.; Sergio, B.N.; Rosado Castellano, P.; Romero Subirón, F. A Tool Condition Monitoring System Based on Low-Cost Sensors and an IoT Platform for Rapid Deployment. *Processes* **2023**, *11*, 668.
11. Zhou, Y.; Kumar, A.; Parkash, C.; Vashishtha, G.; Tang, H.S.; Xiang, J.W. A novel entropy-based sparsity measure for prognosis of bearing defects and development of a sparsogram to select sensitive filtering band of an axial piston pump. *Measurement* **2022**, *203*, 111997. [CrossRef]
12. Gao, C.; Xue, W.; Ren, Y.; Zhou, Y.Q. Numerical Control Machine Tool Fault Diagnosis Using Hybrid Stationary Subspace Analysis and Least Squares Support Vector Machine with a Single Sensor. *Appl. Sci.* **2017**, *7*, 346. [CrossRef]
13. Cao, X.C.; Chen, B.Q.; Yao, B.; He, W.P. Combining translation-invariant wavelet frames and convolutional neural network for intelligent tool wear state identification. *Comput. Ind.* **2019**, *106*, 71–84. [CrossRef]
14. Arellano, G.; Terrazas, G.; Ratchev, S. Tool wear classification using time series imaging and deep learning. *Int. J. Adv. Manuf. Technol.* **2019**, *104*, 3647–3662. [CrossRef]
15. Mohanraj, T.; Shankar, S.; Rajasekar, R.; Sakthivel, N.R.; Pramanik, A. Tool condition monitoring techniques in milling process—A review. *J. Mater. Res. Technol.* **2020**, *9*, 1032–1042. [CrossRef]
16. Zhou, Y.Q.; Zhi, G.F.; Chen, W.; Qian, Q.; He, D.; Sun, B.; Sun, W. A New Tool Wear Condition Monitoring Method Based on Deep Learning under Small Samples. *Measurement* **2022**, *189*, 110622. [CrossRef]
17. Milind, S.; Vinay, V.; Rakesh, C.; Vora, J.; Pimenov, D.Y.; Giasin, K. Tool wear prediction in face milling of stainless steel using singular generative adversarial network and LSTM deep learning models. *Int. J. Adv. Manuf. Technol.* **2022**, *121*, 723–736.
18. Zhou, Y.Q.; Kumar, A.; Parkash, C.; Vashishtha, G.; Tang, H.S.; Glowacz, A.; Dong, A.; Xiang, J.W. Development of entropy measure for selecting highly sensitive WPT band to identify defective components of an axial piston pump. *Appl. Acoust.* **2023**, *203*, 109225. [CrossRef]
19. Xu, Z.; Guo, D.; Wang, J.; Ge, D. A numerical simulation method for a repairable dynamic fault tree. *Eksploat. Niezawodn.—Maint. Reliab.* **2021**, *23*, 34–41. [CrossRef]
20. Zhu, Q.S.; Sun, B.T.; Zhou, Y.Q.; Sun, W.F.; Xiang, J.W. Sample Augmentation for Intelligent Milling Tool Wear Condition Monitoring Using Numerical Simulation and Generative Adversarial Network. *IEEE Trans. Instrum. Meas.* **2021**, *70*, 3516610. [CrossRef]
21. Xiang, J.W.; Zhong, Y.T. A novel personalized diagnosis methodology using numerical simulation and an intelligent method to detect faults in a shaft. *Appl. Sci.* **2016**, *6*, 414. [CrossRef]
22. Gao, Y.; Liu, X.Y.; Xiang, J.W. FEM Simulation-Based Generative Adversarial Networks to Detect Bearing Faults. *IEEE Trans. Ind. Inform.* **2020**, *16*, 4961–4971. [CrossRef]

23. Zakaria, A.M.T.; Thien, D.; Agnes, M.S.; Songmene, V. Numerical Prediction of the Performance of Chamfered and Sharp Cutting Tools during Orthogonal Cutting of AISI 1045 Steel. *Processes* **2022**, *10*, 2171.

24. Reda, A.A.; Abdulrahman, A. Finite Element and Neural Network Models to Forecast Gas Well Inflow Performance of Shale Reservoirs. *Processes* **2022**, *10*, 2602.

25. Shrot, A.; Bäker, M. Determination of Johnson–Cook parameters from machining simulations. *Comput. Mater. Sci.* **2012**, *52*, 298–304. [CrossRef]

26. Chawla, N.V.; Bowyer, K.W.; Hall, L.O.; Kegelmeyer, W.P. SMOTE: Synthetic minority over-sampling technique. *J. Artif. Intell. Res.* **2002**, *16*, 321–357. [CrossRef]

27. Zheng, M.; Wang, F.; Hu, X.W.; Miao, Y.H.; Cao, H.; Tang, M.J. A Method for Analyzing the Performance Impact of Imbalanced Binary Data on Machine Learning Models. *Axioms* **2022**, *11*, 607. [CrossRef]

28. Lei, Z.; Zhu, Q.S.; Zhou, Y.Q.; Sun, B.T.; Sun, W.F.; Pan, X.M. A GAPSO-Enhanced Extreme Learning Machine Method for Tool Wear Estimation in Milling Processes Based on Vibration Signals. *Int. J. Precis. Eng. Manuf. Green Technol.* **2021**, *8*, 745–759. [CrossRef]

29. Duan, C.Z.; Dou, T.; Cai, Y.J.; Li, Y.Y. Finite Element Simulation and Experiment of Chip Formation Process during High Speed Machining of AISI 1045 Hardened Steel. *Int. J. Recent Trends Eng.* **2009**, *1*, 46–50.

30. Tamizharasan, T.; Kumar, S. Optimization of cutting insert geometry using DEFORM-3 D: Numerical simulation and experimental validation. *Int. J. Simul. Model.* **2012**, *11*, 65–76. [CrossRef]

31. Iqbal, S.A.; Mativenga, P.T.; Sheikh, M.A. Characterization of machining of AISI 1045 steel over a wide range of cutting speeds. Part 1: Investigation of contact phenomena. *Proc. Inst. Mech. Eng. Part B J. Eng. Manuf.* **2007**, *221*, 909–916. [CrossRef]

32. Ying, Z.; Keong, K.C. Fast Leave-One-Out Evaluation and Improvement on Inference for LS-SVM's. *Proc. ICPR* **2004**, *3*, 494–497.

33. Gu, J.X.; Albarbar, A.; Sun, X.; Ahmaida, A.M.; Gu, F.; Ball, A.D. Monitoring and diagnosing the natural deterioration of multi-stage helical gearboxes based on modulation signal bispectrum analysis of vibrations. *Int. J. Hydromech.* **2021**, *4*, 309–330. [CrossRef]

34. Govind, V.; Kumar, R. An effective health indicator for the Pelton wheel using a Levy flight mutated genetic algorithm. *Meas. Sci. Technol.* **2021**, *32*, 094003.